

## Dimensional Effects in Micro- and Nanostructural Changes in Grain and Intragrained Structure of Steel 45 at Static-pulse Treatment

A.V. Kirichek<sup>1</sup>, A.P. Kuzmenko<sup>2</sup>, D.L. Soloviev<sup>3</sup>, S.V. Barinov<sup>3</sup>, A.Yu. Altukhov<sup>2</sup>, S.A. Silantiev<sup>3</sup>,  
A.N. Grechukhin<sup>2</sup>, Myo Min Than<sup>2</sup>, M.B. Dobromyslov<sup>4</sup>

<sup>1</sup> Bryansk State Technical University, 7, Bulvar 50-letiya Oktyabrya, Bryansk, Russia

<sup>2</sup> South-West State University, 94, 50 let Otyabrya Str., 305040 Kursk, Russia

<sup>3</sup> Murom Institute (branch) of Vladimir State University by A.G. and N.G. Stoletov,  
23, Orlovskaya Str., Murom, Russia

<sup>4</sup> Pacific National University, 136, Tikhookeanskaya St., Khabarovsk, Russia

(Received 29 September 2015; published online 10 December 2015)

Conducted macro-, micro- and nanostructured materials were investigated by the influence of sample sizes of steel 45 in the form of a parallelepiped, after intense static pulse processing in plastic deformation as in the single (150 J), and pulsed (25 J) impact with a frequency of 23 Hz. When all modes of processing bulk samples found structuring self-organized formation of dislocations. With a single exposure revealed as filling pearlite grains periodic dislocations (200 nm), and the formation of dislocation-free regions. When a periodic pulse treatment of the samples with transverse dimensions fold speed of propagation of elastic waves and shock waves as well as the related transport velocity of dislocations turns shockwave mechanism causing the formation of alternating strips of ferritic and pearlite walls (25 microns), wherein the pearlite wall completely or partially filled with dislocations.

**Keywords:** Plastic deformation, Static-pulse deformation, Shock-wave mechanism, The size effect, Self-organization of dislocations.

PACS numbers: 62.20.F – , 81.40. – z

### 1. INTRODUCTION

Among a wide variety of effective methods to increase strength parameters of metals, alloys and products from them, which is attained by electrophysical, ultrasonic, thermal and chemical heat treatment, essential place is taken by the surface and plastic deformation (SPD) whose variety is the static-pulse treatment (SPT) [1]. In SPT both surface deformation, and its distribution through depth up to the sizes of the processed samples is successfully combined. The growth of hardness observed after such treatment (up to 6.5 GPa) can be due only to occurring volume structural changes.

The physical mechanisms establish interrelations of durability and plasticity of the materials with reorganization of structure under the influence of the shock waves (SWs) excited in the process of SPD [2]. In doing so, all possible channels of elastic energy dissipation are considered: dynamic recrystallization, disclination rearrangement, phase transformations and release of the latent heat of the deformation origin. It should be noted that for localization of the place and time of origin of a defect at SPD, it is required to have spatial-time resolution of up to  $10^{-14}$  s and  $10^{-9}$  m, which is actually difficult to implement. In this regard, authors [3] experimentally have shown 250 fs time resolution in the transmission electron microscope reached without scanning. The analysis of phase transformations  $\gamma \rightarrow \epsilon \rightarrow \alpha$  allowed one to measure by the transmission electron microscopy of high resolution the interplanar shifts caused by SPD [4] in martensite steel. Transitions between individual ones of the presented mechanisms are determined by parameter  $T_{MPD}/T_{melt}$ , i.e. by the ratio of  $T_{MPD}$  – mega plastic deformation (MPD) temperature and  $T_{melt}$  – melting

temperature, which are considered in [5]. A special role of the structure of a surface layer in which local concentrators of tension are formed is emphasized in [6].

In this work the results are presented of nano dimensional investigations of how dimensional factors influence deformation and volume structural changes along the direction of deformation at identical SPT on steel 45 samples in the form of a parallelepiped with multiply changeable sizes.

### 2. PROCESSING TECHNIQUE, METHODS, THE INVESTIGATION RESULTS AND DISCUSSION

Samples from steel 45 in the form of plates with a length of 150, 100 and 50 mm, and also the multiple sizes on width and thickness – 40, 20 and 10 mm have been investigated. All plates were deformed in the middle along the plate length. A roller with a length of 7 and a diameter of 10 mm was used as an impact tool to which an impulse from a striker-wave guide system was transferred. Constant static pressure (about  $10^8$  Pa) plastically deformed the samples, and the subsequent pulse shock action (duration  $\sim 3 \times 10^{-5}$  s) with an energy of 25 J at a striker's speed of 6 m/s increased pressure to 20 GPa. Pulse repetition rate was  $\sim 23$  Hz [1]. SPT was also studied at a single plastic deformation (PD) with a ball (diameter of 19 mm), with an energy of 150 J when pressure up to  $1.4 \times 10^{10}$  Pa was attained. In all cases along the SPT direction, microsection was made for studying phase and structural changes (Fig. 1a).

The metallographic analysis of the structure of the microsection surface was carried out either with the Omega Scope AIST-NT (0.5  $\mu$ m) Confocal microscope

(CM) or the scanning electron microscope (SEM) JEOL JSM-6610 (3 nm). Thus, developed panoramic images of structural changes throughout thickness were obtained: at a macroscopic level with magnification  $\times 505$  every 1 mm, also at a microscopic level –  $\times 2830$  every 300 microns (Fig. 2). In all (macro - and micro) CM images, SPT was directed from right to left. SEM-images are obtained on secondary scattered electrons with a spatial resolution of up to 10 nm.

According to CM (2830 $\times$ ), the structure of the samples studied in the raw state on macro- and microscopic levels was typical for steel 45 and had, in equal parts, ferritic area (F – light) and perlite area (P – dark) (Fig. 1b). After SPT the size of F is significantly reduced due to growth of P grains, and F structure, besides a continuous bordering of perlite grains, penetrated P areas with strip structures. In the microstructure at all CM images in points according to Fig. 1a, the influence of the propagation direction of a spherical shock wave is not established, which is illustrated in Fig. 1e, f, obtained along the axis of impact and at an angle of 45° to it. It should be noted that unlike initial F and P structures (Fig. 1d) after SPT in P grains the ultra-disperse structure presented by formations of martensite, a troostite and sorbite arose. Such changes of steel 45 structure after high-intensity SPT occurred at all depths, which is shown on the CM images (Fig. 1e, f, and also their series in Fig. 2a, b, at different depths).

More detailed structural changes in these conditions are found according to SEM (Fig. 1b, c). So in a near-surface layer directly under SPT point, the characteristic distance between separate structural elements was less than 100 nm. In the points under an impact surface, these elements take a form of strips with a thickness from minimum (less than 100 nm) and to 800 nm with the maximum length of up to 8 microns. Strip curvilinear structures (twins) in P grains are joint in blocks in which they are oriented in parallel among themselves, possessing a sufficient regularity with a minimum period of less than 200 nm. The orientation of strip curvilinear structures in different blocks can vary within  $\pm 45^\circ$ . It is especially noticeable in the points chosen under angles to the direction of shock influence, in particular, as it is shown in Fig. 1c.

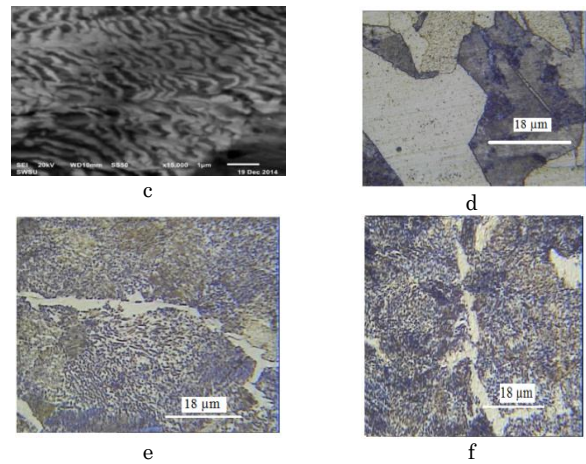
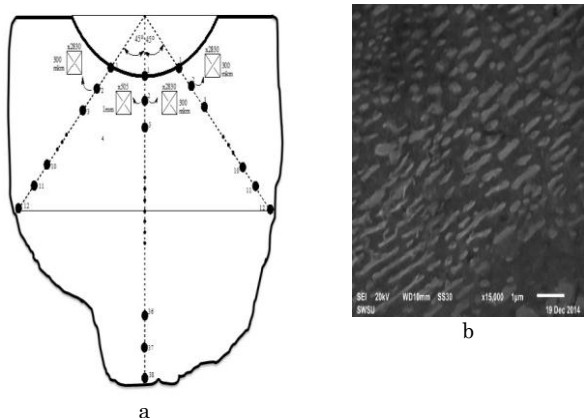


**Fig. 1** – A single shock impulse of SPT on steel 45: a – the micro section; nanostructural SEM images: b – on the impact axis and c – at an angle of 45°; CM microimages: d – without treatment; e – after treatment in the center of a sample along the impact axis, f – on the right under 45°

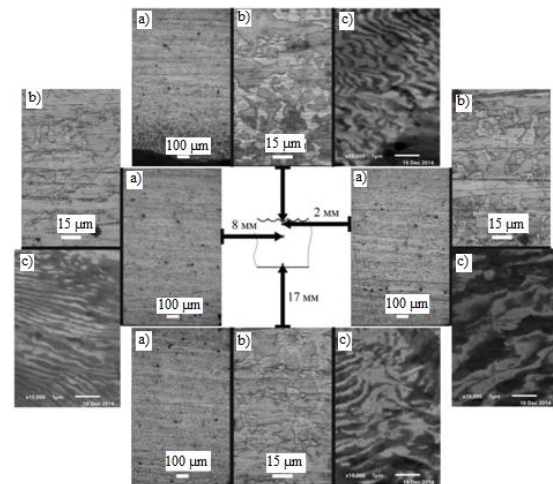


**Fig. 2** – Macro – ( $\times 505$  – a), micro ( $\times 2830$  – b) CM – and nanostructural SEM-images ( $\times 15000$  – c) of the microsection of a steel 45 sample ( $50 \times 20 \times 10$ ) at SPP near the surface and under it: 2, 8 and 17 mm

Structural changes in samples in the form of rectangular rods with different sizes after SPT (25 J, 23.3 Hz) can be subdivided qualitatively in: I – the alternating strip structures formed of F and P components (for samples with sizes of  $50 \times 20 \times 10$ ,  $100 \times 20 \times 10$ ,  $100 \times 10 \times 15$  mm, Fig. 3a-c); II – the alternating strip structures formed from ferritic and perlite (dominating) components. In doing so, the perlite structure either completely, or partially is filled with twins ( $50 \times 10 \times 20$ ,  $100 \times 10 \times 15$  mm, Fig. 3d); III – perlite grains are partially filled with twins ( $50 \times 10 \times 10$ ,  $50 \times 10 \times 10$ ,  $50 \times 20 \times 20$ ,  $150 \times 10 \times 20$  mm, Fig. 3e); IV – the structure of grains did not undergo change ( $5 \times 10 \times 40$ ,  $100 \times 10 \times 10$ ,  $150 \times 20 \times 10$ ,  $150 \times 20 \times 15$ ,  $150 \times 10 \times 10$  mm, Fig. 3f). For structures of the IV type, the areas taken by ferritic and perlite components remain equal. Typical CM images of the rearrangements found are given in Fig. 3. CM images in Fig. 3a, b, c corresponded to mesoscopic structures of the I type in the form of the

alternating strips F and P components which were oriented perpendicular to the shock wave direction. With a rod width of 20 mm, strips F structures dominated, and at its reduction to 10 mm and growth of thickness to 15 mm the area occupied by P structures a little exceeded F (see Fig. 3a, b and Fig. 3c). It is characteristic that the distances between the alternating strips of P and F for I and II types of structures were rather close (about 25  $\mu\text{m}$ ).

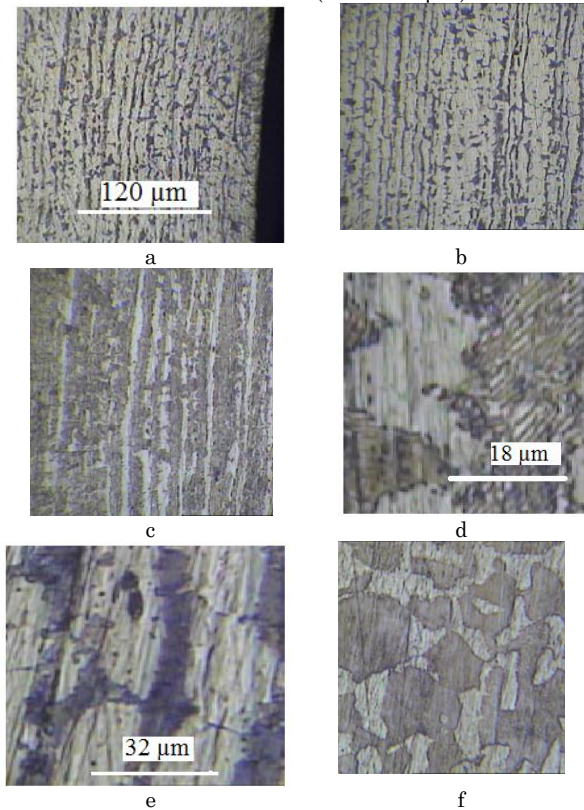


**Fig. 3** – CM images of types of structuring for steel 45 at SPT (25 J, 23.3 Hz, and impact from right to left). I type: a – with a surface of impact and b – (100 × 20 × 10 mm), e – (100 × 10 × 15 mm), II type: c, d – (50 × 10 × 20 mm), f – III (150 × 20 × 10 mm)

Unlike I P structures, the structures of the II type at the microscopic level had twins (Fig. 3d, f); the distance between them, as seen in Fig. 3, reached ~ 4  $\mu\text{m}$ . It is characteristic that twinning structures were oriented either along the SW direction, or at an angle to it. Twinning at SPT occurred also in rods with structural changes of the III type in which strip structures were not formed. However, they were partially or completely filled P areas. Orientation of twinning structures in each perlite grain was either identical, that is single block one, or in it several blocks with excellent orientation were formed. The most detailed idea of these changes was provided by SEM research on all studied rods after SPT. As an example, they are given in Fig. 1b, c and series of images at different depths after SPT of Fig. 2c. In all samples the twinning structures found were characterized by the general regularities. Change of the direction of twins in separate blocks, and also changes of distance between them depending on sample thickness is noted. So, for samples with a thickness of 10 mm, the period of twins

repetition was ~ 170 nm whereas for samples with a thickness of 20 mm it exceeded ~ 400 nm.

The X-ray phase analysis (XRPA) was carried out on the EMMA installation (60 kV, 80 mA, 3 kW, Cu  $K_{\alpha}$ , 1.54  $\text{\AA}$ ). According to XRPA, in the range of  $2\theta = 40\div 90^\circ$  after SPT of samples with different sizes, changes in the reflexes characteristic of steel 45, the most typical of which are brought in Table 1, were found. Here, for comparison the XRPA reference values for steel 45, according to the PDF2 base are presented. In the specified range of angles  $2\theta$ , diffractogram for steel 45 is presented by 3 lines from the planes (110), (200) and (211). After SPT of samples with sizes (150 × 40 × 20), (150 × 40 × 10), (150 × 20 × 10), (100 × 20 × 10), (50 × 20 × 20) and (50 × 20 × 10) besides lines (Table 1), characteristic of steel, reflexes appeared on  $2\theta = 43.410\div 43.467$  and  $50.525\div 50.654$ . The intensity of these lines turned out to be 10 times less than of the main lines. In the same samples, the change of lattice parameters on the main lines is observed, which was up to 0.2 %. It should be noted that in samples with sizes (50 × 40 × 20), (50 × 40 × 10), and (100 × 20 × 20) after SPT new peaks did not arise, and changes of constant lattices were minimum.

**Table 1** – XRPA data of steel 45 samples after SPT

Sample size, mm	$2\theta$ , deg	Lattice constant, $\text{\AA}$	$I$ , arbitrary units	FWHM, $\Delta\theta$ , deg
Standard st. 45	44.7643(110)	2.0229	999	
	65.1641(200)	1.4304	117	
	82.5283(211)	1.1679	180	
50 × 40 × 10	44.790	2.0218	653	0.249
	65.151	1.4306	47	0.307
	82.419	1.1692	79	0.307
150 × 20 × 10	43.410	2.0828	26	0.404
	44.751	2.0235	567	0.269
	50.589	1.8028	16	0.320
	65.092	1.4318/1.4325	50	0.320
	82.393	1.1695	88	0.323

According to Table 1, high-quality comparison of the ratios  $\text{FWHM}(200)/\text{FWHM}(110)$  and  $\cos(2\theta(200))/\cos(2\theta(110))$  showed their proximity, which is indicative of the dominating role of microtensions in the course of SPT, a so-called pining. It is partly explained also by insignificance of changes in constant lattices, unlike crystallites. The strongest change of width of diffraction reflexes at the level of 0.5 is observed along the plane (110) (Table 1), which coincides with the sliding plane for iron along which there is a texturing (pining) of samples. The changes of reflexes after SPT of steel 45 both with consideration for the intensity and their width at half maximum FWHM ( $B$ ) on the basis of the Selyakov-Sherera formula:  $L = k\lambda / B\cos\theta$  allows one to estimate the average size of areas of coherent dispersion ( $L$ ) X-ray radiation ( $\lambda$ ) whose role are played, probably, by textural changes. At constant  $k = 0.94$  for an angle  $\theta$  that corresponds to the main reflex (110), this value was about 180 ~ nm, i.e. practically coincided with the sizes of structures according to SEM (Fig. 1b, c and 2c).

Let's discuss the emergence at SPT in samples of steel 45 alternating strips of P and F oriented

perpendicular to the SW direction (Fig. 3). The amount of pressure upon samples both preliminary and pulsed did not surpass the fluidity limit of Hugoniot, i.e. the samples were not heated at an impact, although a local adiabatic warming was not excluded. In the conditions of SPT, the kinetics of PD ( $U$ ) should be described as relaxation process in which PD in separate points have to be considered [8, 9]:  $\sigma_{ij,j} = \rho d^2 U_i / dt^2$  and variations in corresponding internal rotation moments:  $\varepsilon_{ijk} \sigma_k + \mu_{ij,j} = J_{ji} d^2 \omega_i / dt^2$ . Here  $\varepsilon_{ijk}$  is the Levi-Civita tensor,  $J_{ji}$  is the moment of inertia considering turns of points of the environment at rotation with a frequency  $\omega_i$ ,  $U$  is corresponding translation. In doing so, at an early stage of deformation (at  $t_1$ ) only PD occurred, and further at  $t_2$  there are already torsion bending deformations. The structural rearrangements arising at SPT with the specified parameters in the steel 45 studied can be described by the following equation with respect to  $U$ :  $(\lambda + \mu) \partial(\text{div} U) / \partial x_i + \mu \Delta U - 3\alpha K \partial T / \partial x_i = \rho \partial^2 U / \partial t^2$ . Here  $x_i = X, Y, Z$  are coordinates,  $T$  is temperature,  $\lambda$  and  $\mu$  are the Lamé coefficients,  $\rho$  is the material density,  $\alpha$  is the coefficient of thermal expansion,  $K$  is the module of volume compression,  $\text{div} U$  considers the movements of defective formations at PD both in the form of translations and torsions and bends.

The resulting speed of the SW at PD approaches the speed of volume sound waves for steel 45: transversal  $V_t = 3 \times 10^3$  m/s and longitudinal –  $V_l = 6 \times 10^3$  m/s. At SPT the PD dominates. Elastic deformation manifests itself only at the initial ( $t_0$ ) and final ( $t_c$ ) processing stages. PD occurs within  $t_c > t > t_0$ , which coincides with a duration of an impact pulse  $\tau = 10^{-5}$  s. This fact made it possible to determine the distance of SW propagation both along and across the direction of the influence, which amounted to 3 and 6 cm, respectively. The samples studied had the cross sizes less than distances of SW propagation. According to [2], transfer of pressure ( $P$ ) at SW propagation can be described by

mass speed:  $V = P / (V_l \rho) \sim 500$  or 300 m/s, where density of steel  $\rho \sim 8 \times 10^3$  kg was accepted invariable. At such speeds of changes  $P$  at impact of SWs with consideration for  $\tau$ , they, at a single impact, will go  $S_l = 3$  and  $S_t = 5$  mm, respectively. This fact explains the absence of strip F and P structures at a single impact (Fig. 1f). Whereas when samples of steel 45 are treated with a frequency of SWs  $f \sim 23$  Hz, when their cross sizes become multiple to these distances of  $S_l$  and / or  $S_t$  of transfer of changes  $P$ , conditions for modulation of density of both  $dU / dt$  – translational dislocations, and  $d\omega_i / dt$  – deformations of torsion and bending or disclinations are created. Check of the estimates made can be carried out only for longitudinal SWs, i.e. on the microsection along thickness of a lamellar steel 45 sample, on macro- micro and nanostructural variations (Figs. 1-3). With consideration for the average size of strip structures of 25  $\mu\text{m}$  (Figs. 2a and 3a-c) in the analysis of their entire panorama along the micro-section, the number of the strip dislocation structures distributed throughout thickness of 15 mm, coincided with the calculated one.

Thus, at deformation under conditions of both elastic harbinger and at the initial site of SW at PD, the heterogeneous mechanism of self-organized formation of dislocations operates. At a single SW, a nanodimensional dislocation structure in each grain with a minimum period of less than 200 nm occurs. At deeper PD under the influence of repeated SWs, the density of dislocations considerably increases, and also there is a formation of dislocation walls (Fig. 3a-c) under the influence of the shock and wave modulation mechanism.

## ACKNOWLEDGEMENTS

The reported study was funded by RFBR according to the research project No 14-08-00112 A.

## REFERENCES

1. A.V. Kirichek, D.L. Soloviev, A.G. Lazutkin, *Technology and equipment of static-pulse treatment with surface plastic deformation* (M.: Mashinostroyeniye: 2004) [In Russian].
2. V.E. Panin, V.E. Egorushkin, *Phys. Mesomechanic.* **16**, 267 (2013).
3. S.G. Psakhe, K.P. Zolnikov, D.S. Kryzhevich, A.N. Tyumentsev, *Phys. Mesomechanic.* [In Russian].
4. V. Novatskiy, *The elasticity theory* (M.: Mir: 1975) [In Russian].
5. P.V. Makarov, *Physics of burning and explosion* No 1, 22 (1987) [In Russian].